The 3-D Plasma Distribution Function Analyzers With Time-of-Flight Mass Discrimination for Cluster, FAST, and Equator-S

E. Möbius[1], L.M. Kistler[1], M.A. Popecki[1], K.N. Crocker[1], M. Granoff[1], Y. Jiang[1], E. Sartori[1], V. Ye[1], H. Réme[2], J.A. Sauvaud[2], A. Cros[2], C. Aoustin[2], T. Camus[2], J.-L. Médale, J. Rouzaud[2], C.W. Carlson[3], J.P. McFadden[3], D. Curtis[3], H. Heetderks[3], J. Croyle[3], C. Ingraham[3], B. Klecker[4], D. Hovestadt[4], M. Ertl[4], F. Eberl[4], H. Kästle[1,4], E. Künneth[4], P. Laeverenz[4], E. Seidenschwang[4], E.G. Shelley[5], D.M. Klumpar[5], E. Hertzberg[5], G.K. Parks[6], M. McCarthy[6], A. Korth[7], H. Rosenbauer[7], B. Gräve[7], L. Eliasson[8], S. Olsen[8], H. Balsiger[9], U. Schwab[9], M. Steinacher[9]

A similar time-of-flight plasma analyzer system will be flown as CODIF (COmposition and DIstribution Function analyzer) on the four Cluster spacecraft, as ESIC (Equator-S Ion Composition instrument) on Equator-S, and as TEAMS (Time-of-flight Energy Angle Mass Spectrograph) on FAST. These instruments will for the first time allow the 3-dimensional distribution functions of individual ion species to be determined within 1/2 or 1 spin period. This will be crucial for the study of selective energization processes in various regions of the magnetosphere. The sensor consists of a toroidal top-hat electrostatic analyzer with instantaneous acceptance of ions over 360° in polar angle. For Cluster and Equator-S this range is subdivided into two halves with geometric factors different by a factor of 100 in order to cope with the wide dynamic range of fluxes in the magnetosphere. For FAST the time resolution is increased by a factor of two to focus on fast auroral phenomena by using both halves simultaneously. After post-acceleration of the incoming ions by up to 25 kV, a time-of-flight mass spectrograph discriminates the individual species. It has been demonstrated in calibration runs that the instruments can easily separate H^+, He^{2+}, He^+, O^+ and for energies after post-acceleration of ³ 20 keV even O_2^+ molecules. On board discrimination, accumulation, and moment computation allow efficient retrieval of the data stream.

[1]Institute for the Study of Earth, Oceans and Space, University of New Hampshire, Durham, NH 03824
[2]Centre d'Etude Spatiale et Rayonnement, B.P. 4346, F-31029 Toulouse Cedex, France
[3]Space Sciences Laboratory, University of California Berkeley, CA 94720
[4]Max-Planck-Institut für extraterrestrische Physik, Pastfach 1603, D-5740 Garching, Germany
[5]Lockheed-Martin Palo Alto Research Laboratory, 3251 Hanover St., Palo Alto, CA 94304
[6]Space Program, University of Washington, Seattle, WA 98195
[7]Max-Planck-Institut für Aeronomie, Postfach 20, D-37189 Katlenburg-Lindau, Germany
[8]Institut for Rømdfysik, P.O. Box 812, S-98128 Kiruna, Sweden
[9]Physikalisches Institut der Universität Bern, Sidlerstr. 5, CH-3012 Bern, Switzerland

Measurement Techniques in Space Plasmas: Particles
Geophysical Monograph 102

INTRODUCTION

After the application of time-of-flight (TOF) mass-spectrographs in space had been successfully pioneered with the AMPTE mission in 1984 (Gloeckler et al., 1985; McEntire et al., 1985; Möbius et al., 1985) TOF instruments have become a standard tool in space plasma physics. TOF instruments have been flown in different configurations on missions, such as Viking, Giotto, VEGA, Phobos, Ulysses, and the GGS spacecraft. The ion composition results from these missions has clearly demonstrated the excellent capabilities of this type of instrumentation in both the energy range of the bulk plasma as well as in the energy gap

between about 30 keV and several hundred keV/nucleon, which existed between the regimes of magnetic mass spectrographs and cosmic ray telescopes.

More recently the further evolution of this type of instrument has branched into two directions to optimize their use for different applications. Along one line the mass resolution of this class of instruments has been substantially enhanced by the introduction of isochronous TOF spectrographs (Hamilton et al., 1990; Möbius et al., 1990). Such spectrographs are on Wind, SOHO (Hovestadt et al. 1995) and Cassini (McComas et al., 1997). In another effort to simultaneously determine the 3-dimensional distribution function separately for the main ion species, the concept of the fast 3-D plasma instrument on AMPTE/IRM (Paschmann et al., 1985) has been combined with the TOF technique and post-acceleration for the ESA/NASA Cluster mission (Rème et al., 1993). Similar instruments will be flown on FAST (Carlson, 1992) and on Equator-S. The major achievement of these instruments will be to allow the accumulation of full velocity distribution functions for 4 major species (e.g., H^+, He^{2+}, He^+ and O^+) within 1 spacecraft spin on Cluster and Equator-S or within 1/2 spin period on FAST. The instantaneous coverage of a two-dimensional cut of the distribution function is achieved within one energy sweep whose typical duration is 60 - 250 msec. This capability will significantly enhance our knowledge of the dynamics in multi-ion plasmas.

INSTRUMENT DESCRIPTION

The instrument combines the selection of incoming ions according to energy per charge by electrostatic deflection in a toroidal analyzer with post-acceleration by up to 25 keV/e and subsequent TOF analysis as shown in Figure 1.

The instrument is mounted with its axis of symmetry perpendicular to the spacecraft spin axis. The front end of the sensor is protruding out of the spacecraft surface so that its 360° aperture has a free field-of-view. The electrostatic analyzer (ESA) is of a toroidal top-hat type with a uniform response over 360° of polar angle. As illustrated in Fig. 1, the analyzer consists of an inner toroid, to which a variable negative potential is applied, an outer toroid with a cut-out at the top, and a top-cap lifted above the outer toroid. Both, the outer toroid and the top-cap are normally held at ground potential, thereby exposing no high voltage to the outside world. A beam of parallel ion trajectories entering the aperture is focused to a certain location at the exit plane of the analyzer. This location determines the incident polar angle of the ions. With a cross-plate voltage of 2-5200 V (varied with logarithmically spaced steps), the energy range is 15-40000 eV/e for CODIF and ESIC. The corresponding numbers are 0.6-1300 V with an energy range of 5-12000 eV/e for TEAMS. The analyzer has an intrinsic energy

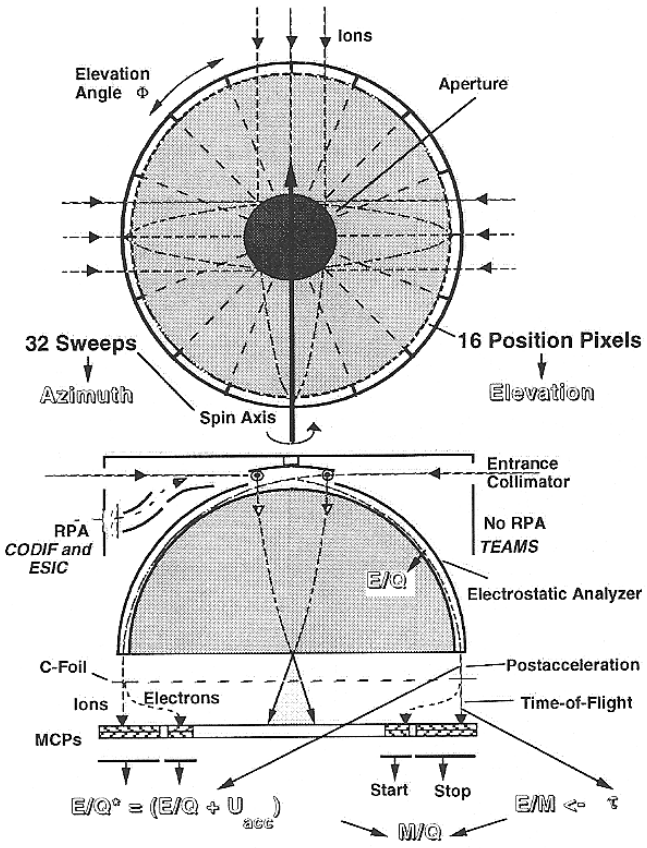

Figure 1. Schematic view of the sensor and its operational principles in a top view and a cross-sectional view of the sensor. The electrostatic analyzer is of a toroidal type.

resolution of $\Delta E/E \approx 0.13$. It is surrounded by a cylindrical collimator which serves to define the acceptance angles. The full polar angle of the analyzer is divided into 16 pixels of 22.5° each. The full energy sweep will be performed 32 times per spin. Thus a two dimensional cut through the distribution in polar angle with 11.25° resolution in azimuthal angle is obtained every 1/32 of a spin period. For TEAMS an additional mode with 64 sweeps per spin (5.6° resolution) has been implemented. The geometric factor over one individual pixel is defined as $A \cdot \Delta E/E \cdot \Delta\theta \cdot \pi/8$, where A denotes the aperture area and $\Delta\theta$ the azimuthal width of the analyzer. This value takes into account the transmissivity of all grids and support structures in the sensor. For TEAMS both halves are identical, thus covering the full sphere in half a spin period. The entrance apertures of CODIF and ESIC provide two different geometrical factors in order to maximize the dynamic range of the instruments, with the geometric factor in the second half attenuated by a factor of 100 using an array of pin holes. The values for all sensors are compiled in Table 1.

On Cluster and Equator-S where regions with very low temperature plasma will be encountered, the low-energy portion of the ion distribution (≈ 0-20 eV) is sampled by an additional retarding potential analyzer (RPA) at the entrance of the ESA with a geometrical factor of 0.04 cm^2sr for the

TABLE 1. Instrument Capabilities

Species	Energy Range	ΔE/E	A·ΔE/E·ΔΘ·π/8 (cm^2sr)	Instantaneous Field of View	Angular Resolution	Time Resolution	Mass Power	Power	Mission
H^+, He^{2+},	15eV - 40keV		high $2.16 \cdot 10^{-3}$			1 spin			
He^+, O^+,	RPA:	0.13	low $2.3 \cdot 10^{-5}$	360° x 8°	11.2° x 22.5°	(4 sec)	8.05 kg	7.95 W	Cluster
(O_2^+, NO^+)	S/C Pot - 20eV					(1 sec)	8.49 kg	8.4 W	Equator-S
					5.5° x 22.5°	1/2 spin			
dto.	3 eV - 12 keV	0.13	$1.5 \cdot 10^{-3}$	360° x 8°	11.2° x 22.5°	(2.5 sec)	7.6 kg	4.95W	FAST

full 360° acceptance angle and an aperture area of 0.04 cm^2 for beam distributions. In the RPA mode of the instrument the ions are collected through a separate aperture for the RPA, while the normal aperture is electrically blocked. The ions are pre-accelerated into the ESA to 100 eV/e by setting the outer electrodes to -100 V.

Behind the energy analyzer the ions are accelerated by a voltage of -15 to -25 kV, such that the ions have a minimum energy before entering the TOF section. The energy per charge E/Q as selected by the ESA plus the energy $e \cdot U_{ACC}$ gained by post-acceleration and the measured time-of-flight τ through the length d of the TOF unit are combined into the mass per charge M/Q of the ion according to:

$$M/Q = 2(E/Q + e \cdot U_{ACC})/(d/\tau)^2 \cdot \alpha.$$

The quantity α represents the effect of energy loss in the thin carbon foil ($\approx 3 \mu g/cm^2$) at the entry of the TOF section and depends on particle species and incident energy. A schematic radial cross-section of the TOF system of the sensor with the most important elements is shown in Fig. 2. The start signal is provided by secondary electrons, that are emitted from the carbon foil during the passage of the ions. The electrons are accelerated and deflected onto the start portion of the microchannel plate (MCP) by the appropriate potential configuration. The secondary electrons also provide the position information for the angular sectoring. To allow good angular resolution, a toroidal geometry has been chosen for the analyzer which pushes its focal point close to the carbon foil plane. The carbon foil is made up of 22.5° sectors, separated by narrow metal strips. The electron optics are designed to strongly focus secondary electrons originating at a foil onto the corresponding MCP start sector, using the fringe fields of the radial foil support structures and radial fin separators between the sectors. The MCP assemblies are ring shaped quadrants with radii of 3 by 9 cm which serve both the Start and Stop signals. The signal output of the MCPs consists of a set of segmented plates (22.5° each) behind the start MCP and (90° each) behind the stop MCPs as well as thin wire grids with ≈ 85% transmission at a distance of 10 mm in front of the signal plates, all being at ground potential. The timing information is taken from the grids, while the position signals are taken separately from the segmented plates.

The sensor electronics consists of two time-to-amplitude converters to measure the time-of-flight of the ions between the start C-foil and the stop MCPs separately for two halves of the TOF section, 16 position discriminators at the Start and 4 position discriminators at the Stop section of the MCPs, as well as event selection logic. The TOF for each ion is pulse height analyzed. The incidence in azimuthal (5 bit given by the spacecraft spin) and polar angle (4 bit given by the start position), and the actual deflection voltage (8 bit) are added to the event information. The resulting digital outputs are encoded in a look-up table, and the resulting energy-angle event is accumulated into incrementing memories with variable binning (according to the selected instrument mode) in energy and angle, separately for 4 different masses, or with long accumulation for up to 64 masses. A more detailed description of the electronics may be found elsewhere (Rème et al., 1993).

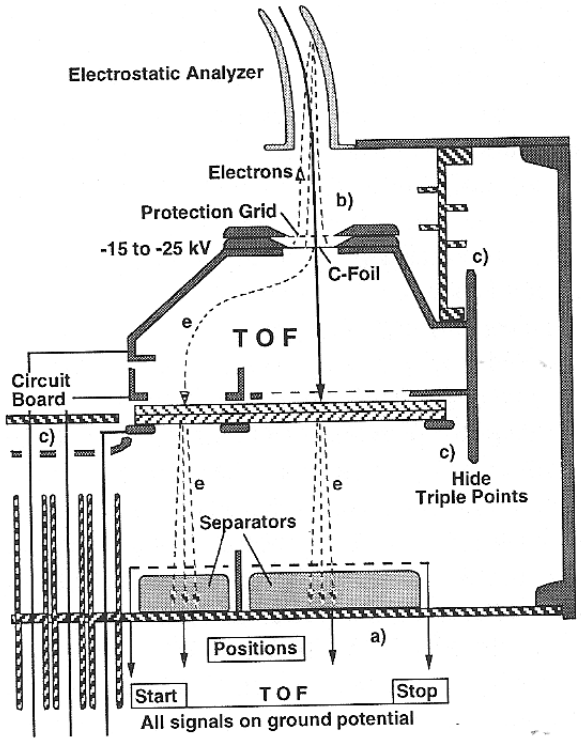

Figure 2. Cross-sectional view of the critical design elements in the TOF section (drawing not to scale). which are emitted from the carbon foil during the passage of the ions.

CRITICAL DESIGN ELEMENTS

Two requirements on the CODIF, TEAMS and ESIC sensors had a large impact on the final design: 1) In order to measure the 3D distribution function with reasonable angular resolution the electrostatic analyzer must image the angular distribution to the carbon foil and the cylindrical TOF section must be divided into at least 16 pixels. 2) In order to provide mass resolution for ions with masses up to 16 (or even 32 for molecular ions) at plasma energies a post-acceleration voltage of at least 15 kV is needed.

The focal plane of quadrispherical analyzers coincides with their exit. Because of the post-acceleration gap the incoming ions would already be divergent in the carbon foil plane where the position is determined. Therefore, a toroidal ESA was chosen. The optimization for this application was reached through careful computer simulations before the final design. A detailed description may be found in a paper by McFadden and Carlson (1997) in this volume.

In order to achieve position resolution with 16 pixels, while minimizing the TOF electronics (a) in Fig. 2, the electron signals were split within the sensor. The Start and Stop signals for the TOF analysis are taken from metallic grids at 10 mm above the position pixels. In this way an almost complete separation of both electronic systems can be achieved except for stray capacitances between the different electrodes. Unipolar signals without overshoot for both timing and position could be achieved with the grid and pixels on exactly the same, i.e. ground, potential. It was derived experimentally that an even split of the signal between both terminals is reached with an ≈ 80-90% transmission grid. This can most probably be attributed to fringing fields near the grid, but this has not been modeled during the design of the instrument. To reduce capacitive cross-talk between adjacent pixels, ground traces with etched CuBe separators soldered to them have been inserted. In this way a suppression of cross-talk to as low as 1% of the original signal height has been achieved.

To provide the necessary post-acceleration the complete interior part of the TOF section, including the MCPs has to be at negative potential (≈ -15 to -25 kV). In order to avoid elaborate high voltage interfaces for the MCP signals the electron cloud that leaves the MCP is accelerated by the post-acceleration voltage to electrodes at ground potential. Thus all signals can be referenced to ground. The only high voltage interfaces are the power connections to the deflection electrodes and the MCPs in the TOF section.

Any conducting surfaces at negative high potential tend to emit electrons. Depending on where these electrons strike a solid surface in the sensor they can contribute substantially to instrument background. For example, secondary electrons emitted by the carbon foil of the TOF section into the direction of the ESA (b) in Fig. 2 may produce secondary ions of gases that are attached to the surface of the ESA or the mounting plate. If created at the exit of the ESA they can be accelerated into the TOF section and thus are identified as ions which cannot be distinguished from natural ions entering the analyzer with very low energies. Therefore, great care has been taken to focus secondary electrons of this kind deep into the ESA. Such focusing becomes almost impossible to achieve for secondary electrons from the edge of the carbon foil where it meets the mounting frame. Unfortunately, it cannot be guaranteed that all 16 foils are perfect throughout all the handling. A tiny rupture next to the edge can therefore provide a strong source of secondary electrons in the post-acceleration electric field. Background increases which could be related to foil damage after the test were observed during sensor operation in the laboratory. Therefore, a second grid (denoted "Protection Grid" in Fig. 2) was added in front of the carbon foil to significantly reduce the electric field at the foil surface. This protection has removed the secondary electron background.

The mounting of the TOF structure with an insulator to the housing, the MCP assembly, and the high voltage connection in the center of the sensor are areas where triple points (junctures of metallic and insulator surfaces exposed to vacuum) cannot be avoided (c) in Fig. 2). These triple points are known as potentially dangerous starting points for electron migration in high voltage environments. Therefore, all unavoidable triple points are either placed in regions with dramatically reduced field strength by field shaping electrodes or hidden under a shield.

TEST AND CALIBRATION RESULTS

A compilation of time-of-flight spectra for the key ion species at 25 keV/charge is shown in Fig. 3. Because the major species in the magnetosphere, ionosphere, and solar wind are separated by factors of 2 in mass/charge a clear

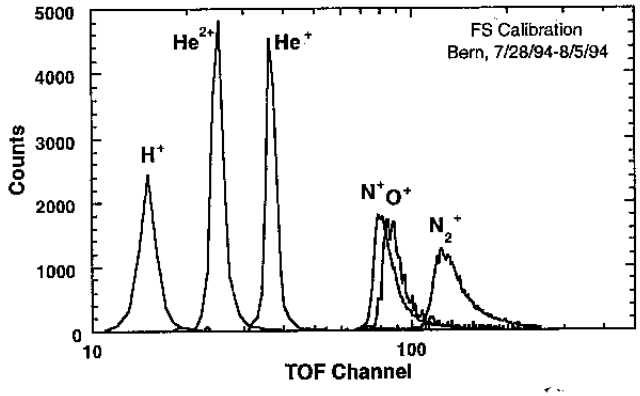

Figure 3. Time-of-flight spectrum for H^+, He^{2+}, He^+, N^+, O^+, and N_2^+, as taken at the calibration facility of the University of Bern with a total ion energy of 25 keV/charge.

identification of these ions even with poorer resolution, i.e. for reduced post-acceleration is possible. Ions adjacent on the mass scale, such as N and O, cannot be easily distinguished. However, this was never a goal for an instrument designed to determine the velocity distribution for the major species that contribute significantly to the dynamics of the plasmas in the magnetosphere and the solar wind.

The calibration of the sensor efficiency for all species and the complete energy range provided another challenge. While the response of an ESA remains essentially unchanged for different species and over the entire energy range, the detection efficiency of TOF assemblies changes with species and energy due to dependencies of the secondary electron production in the C-foils and the sensitivity of the MCPs. Variations due to angular scattering are negligible due to the post-acceleration. To reduce the anticipated variations the MCPs are operated in saturation of their gain. Yet there are still significant variations of the efficiency with species, energy and position on the MCPs that may be as large a factor 2. Therefore, each sensor has been calibrated in a matrix of ion species, energies and MCP position. The variation of the efficiency as a function of energy for a typical sensor model is shown in Fig. 4 for H^+, He^+, and O^+. The decrease of the H^+ efficiency with energy could be attributed to not reaching saturation. This poses no problem for TEAMS ($E \leq 12$ keV). For ESIC and CODIF the transparency of the grid for the stop signal was reduced in a recent effort, which increased the stop signal and raised the efficiency substantially.

First scans of the sensor in the electrostatic analyzer voltage and azimuthal angle had suggested that the TOF section might even introduce a variation of the response in these parameters. Instead of the theoretical ESA response, unanticipated reductions of the detection efficiency were observed as a function of ESA voltage or acceptance angle. However, it was found that the focusing of the incoming ion beam by the post-acceleration field at the TOF entrance is so thin that the support grid structure becomes visible. This effect is not visible for an ion distribution sufficiently wide in angle and energy as can be assumed for realistic conditions. This could be verified by a combined angle and analyzer voltage scan, as shown in Fig. 5. The variation of the response is shown as a function of ESA voltage (in a) and azimuthal angle (in b). In both cases the response has been integrated over azimuthal angle (in a)) and ESA voltage (in b)), respectively. Now the grid structure becomes invisible and the curves closely match the theoretical response of the ESA as has been confirmed in separate calibrations of the ESA assemblies. The remaining effect of the carbon foil support grids is a reduction of the detected flux according to the transmission of the grids that has also been calibrated. The calibration effort for the RPA of this instrument may be found in a paper by McCarthy and McFadden (1997) in this volume.

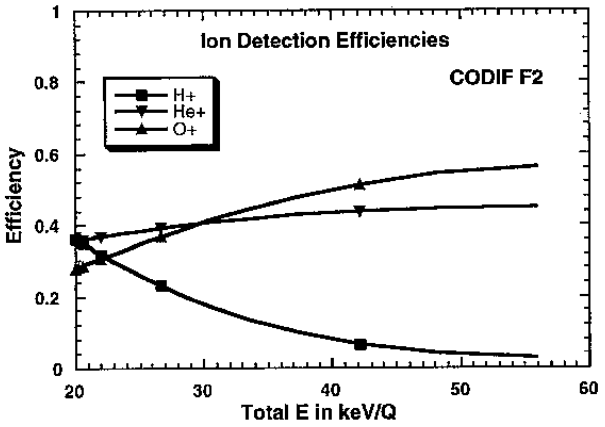

Figure 4. Efficiency of the time-of-flight section as a function of total internal energy for H^+, He^+, and O^+ as measured for a typical sensor model. While the absolute values vary with the models the curves remain similar.

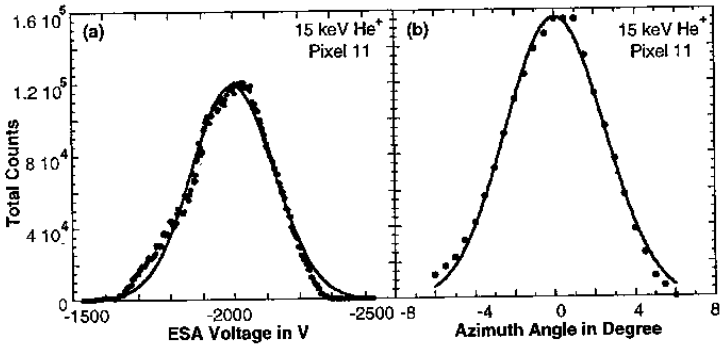

Figure 5. Overall response in Azimuthal Angle (analyzer deflection direction) **(a)** and in Electrostatic Analyzer Voltage **(b)** as measured for the Cluster Flight Spare in comparison with a simulation of the electrostatic analyzer characteristics.

MODULAR CONCEPT

The CODIF, TEAMS and ESIC sensors consist of several self-contained subsystems that can be separately designed built and tested, as outlined in Fig. 6. The subsystems are the electrostatic analyzer, the TOF system that can even be separated into a sensor- and an electronic-module, and the data processing system. Each subsystem can be adapted individually to the requirements of a specific space mission. The instrument capabilities are compiled in Table 1, including the individual differences of the instruments. For all 3 sensors the responsibility for the central TOF subsystem rests with the University of New Hampshire (sensor) and the Max-Planck-Institut für extraterrestrische Physik (electronics). This key system, which has been the centerpiece in the previous chapters, remains identical. The ESA is being provided by CESR, Toulouse, for CODIF

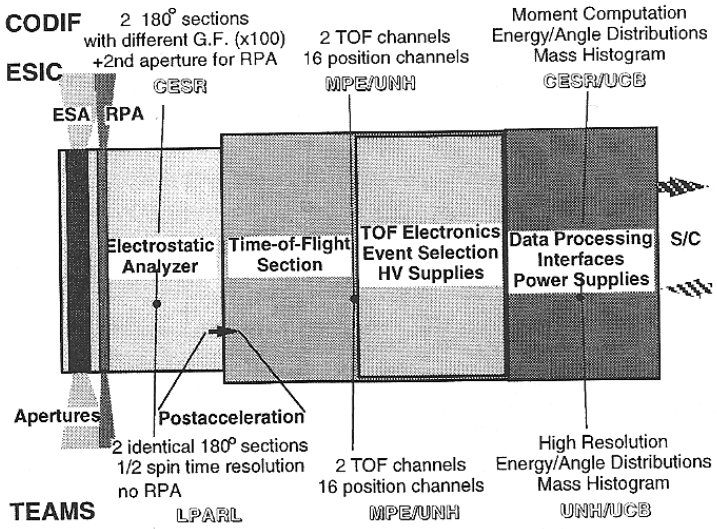

Figure 6. Block diagram of the modular concept of CODIF, TEAMS and ESIC with team responsibilities and modifications for the different missions.

and ESIC and by the Lockheed Martin Palo Alto Research Lab for TEAMS. Cluster and Equator-S will scan regions with a wide dynamic range of fluxes and encounter occasionally very cold plasmas. Therefore, the CODIF and ESIC are equipped with two sections that are different in geometric factor by approximately a factor of 100. For FAST the emphasis is on very high spatial and thus temporal resolution of auroral structure,s and therefore a single geometric factor is chosen for TEAMS allowing twice the time resolution. CODIF and ESIC also carry an additional retarding potential analyzer which extends the energy range to practically 0 eV (spacecraft potential). The RPA is implemented with a separate entrance aperture that is adjacent to the regular ESA aperture. The ions are guided into the ESA by a sequence of deflection plates and grids.

The other profound difference is found in the data processing systems of these instruments. In the case of CODIF and ESIC the data processing system consists of a microprocessor capable of compressing the raw data stream very efficiently by the accumulation of mass, angle and energy bin distributions and computation of the first 3 to 4 moments of the distribution function for four different ion species. The first step allows a compression by a factor of $\approx$ 120. Reduction of the distribution elements by taking into account the oversampling of the sphere at the poles allows another factor of 2.5 in reduction. The moments need only $\approx$ 3% of the original bit stream. These data compression schemes provide for many possible telemetry modes for different environments and data rates. The only differences between CODIF and ESIC are the spacecraft interface circuitry and the on board software which has to cope with a 1 sec spin rate for Equator-S. Because FAST has a large memory capability and will be run in a campaign mode during the aurora passages, a much higher data rate can be offered. Therefore, TEAMS possesses only a data processing interface with storage capability for the mass, angle, energy distributions, which are buffered, before the next voltage sweep starts, and then read out completely during this sweep cycle. TEAMS will allow a tracking of distribution functions with the highest time resolution.

Acknowledgements. The authors are indebted to the many unnamed individuals in the electronic and machine shops as well as administrative and support units at all institutions involved in the hardware implementation. The instruments are supported by NASA for Cluster under NAS5-30613, for FAST under NAS5-31283, and for Equator-S under NAGW-3723, by CNES under Grant 208, and by the Bundesministerium für Forschung und Technologie under FKZ 50 OC 89069 at MPE Garching and FKZ 50 OC 89030 at MPAe Lindau. Calibrations at the Bern facility were supported by the Swiss National Science Foundation.

REFERENCES

Carlson, C.W., The Fast Auroral Snapshot Explorer, *EOS, 73, #23*, 249, June 9, 1992.

Gloeckler, G., et al., The Charge-Energy-Mass spectrometer for 0.3 - 300 keV/e ions on the AMPTE/CCE, *IEEE Trans. on Geosci. and Remote Sens., GE-23*, 234, 1985.

Hamilton, D.C., et al., New-high resolution electrostatic ion mass analyzer using time-of-flight, *Rev. Sci. Instrum., 61*, 3104, 1990.

Hovestadt, D., et al., CELIAS - Charge, Element and Isotope Analysis System for SOHO, in: The SOHO Mission, *Solar Phys., 162*, 441 - 481, 1995.

McCarthy, M., and J.P. McFadden, Measurements of 0-25 eV ions with a retarding potential analyzer on the Cluster Ion Spectroscopy experiment, Geophysical Monograph, this volume, 1997.

McComas, D.J. et al., The Cassini Ion Mass Spectrometer, this volume, 1997.

McEntire, R.W., et al., The Medium-Energy Particle Analyzer (MEPA) on the AMPTE CCE spacecraft, *IEEE Trans. on Geosci. and Remote Sens., GE-23*, 230 , 1985.

McFadden, J.P., and C.W. Carlson, Computer simulation in designing electrostatic optics for space plasma experiments, Geophysical Monograph, this volume, 1997.

Möbius, E., et al., The time-of-flight spectrometer SULEICA for ions of the energy range 5 - 270 keV/charge on the AMPTE/IRM, *IEEE Trans. on Geosci. and Remote Sens., GE-23*, 274, 1985.

Möbius, E., P. Bochsler, A.G. Ghielmetti, D.C. Hamilton, High mass resolution isochronous time-of-flight spectrograph for three-dimensional space plasma measurements, *Rev. Sci. Instrum., 61*, 3609 - 3612, 1990.

Paschmann, G., et al., The plasma instrument for AMPTE/IRM, *IEEE Trans. on Geosci. and Remote Sens., GE-23*, 262, 1985.

Rème, H., et al., The Cluster Ion Spectrometry experiment, *ESA-SP, 1159*, 133 - 162, 1993.